Accident Analysis and Prevention 129 (2019) 263–276

Contents lists available at ScienceDirect

Accident Analysis and Prevention

journal homepage: www.elsevier.com/locate/aap

Transferability of real-time safety performance functions for signalized intersections

Mohamed Essa*, Tarek Sayed, Passant Reyad

Department of Civil Engineering, University of British Columbia, 6250 Applied Science Lane, Vancouver, BC, V6T 1Z4, Canada

ARTICLE INFO

Keywords:
Transferability analysis
Safety performance functions
Traffic conflict analysis
Effect of signal design on safety
Real time safety evaluation

ABSTRACT

Optimizing traffic signals in real-time for safety performance can be executable in the era of Connected Vehicles (CVs) when real-time information on vehicle positions and trajectories is available. To achieve this, real-time safety models are needed to understand how changes in signal controllers affect safety in real-time. Recently, several real-time safety models were developed for signalized intersections that relate various dynamic traffic parameters to the number of rear-end traffic conflicts at the signal cycle level. The traffic parameters included: traffic volume, maximum queue length, shock wave speed and area, and platoon ratio. For wider application of these models to other jurisdictions, the transferability of these models needs to be examined. Therefore, this paper aims to investigate the transferability of several signalized intersections real-time safety models to new jurisdictions. Two corridors of signalized intersections in California and Atlanta were used in the analysis as destination jurisdictions. Detailed vehicle trajectories for these corridors were obtained from the Next Generation Simulation (NGSIM) data. Various transferability analysis approaches were applied. The transferability of the real-time safety models was evaluated with and without a local calibration for the model parameters at the new jurisdictions. Several goodness-of-fit measures were examined to assess the ability of the developed models to predict traffic conflicts. Overall, the results showed that the real-time safety models are transferable, which confirms the validity of using them for real-time safety evaluation of signalized intersections.

1. Introduction

Connected vehicles (CVs) are expected to generate considerable real-time data on vehicle positions and trajectories via wireless communication between vehicles, infrastructure, and other road users (U.S. Department of Transportation, 2015). These data can potentially be used to improve road safety in real-time. Therefore, with the increasing emergence of the CVs technology, there is a growing interest in developing real-time safety models that can utilize CVs data to evaluate traffic safety in real-time. The most important use of these safety models is to predict, evaluate and proactively optimize road safety in real-time.

Recently, several real-time safety models have been developed by researchers for different road facilities, such as freeways (Lee et al., 2003; Pande and Abdel-Aty, 2006; Hossain and Muromachi, 2012; Ahmed and Abdel-Aty, 2013) and signalized intersections (Theofilatos, 2017; Theofilatos et al., 2017; Yuan and Abdel-Aty, 2018; Yuan et al., 2018; Essa and Sayed, 2018a, 2018b). Real-time safety models differ from traditional safety performance functions (SPFs) in two main aspects. First, traditional safety models predict the number of collisions in several years, while real-time safety models can predict the level of safety, such as the crash risk or the number of traffic conflicts, in considerably shorter time periods, usually a few minutes. Second, traditional safety models consider mainly the traffic flow, which is usually aggregated to the annual average daily traffic (AADT), while real-time safety models consider several traffic characteristics and their recurrent variation.

One important issue when developing safety models ——whether real time or not—— is to investigate the transferability of the developed model to new jurisdictions. While considerable research has been conducted on examining the transferability of traditional SPFs (the aggregated SPFs) (Srinivasan and Carter, 2011; Xie et al., 2011; Brimley et al., 2012; Young et al., 2012; Mehta and Lou, 2013; D'agostino, 2014; Cunto et al., 2014; Srinivasan et al., 2016; Farid et al., 2018; among others), a few studies have investigated the transferability of real-time safety models (e.g., Xu et al., 2014; Pande et al., 2011; Shew et al., 2013).

The objective of this study was to investigate the transferability of real-time safety models. In particular, the transferability of the real-time safety models presented in (Essa and Sayed, 2018a) was examined.

* Corresponding author.
E-mail addresses: m.a.essa@civil.ubc.ca (M. Essa), tsayed@civil.ubc.ca (T. Sayed), p_reyad@civil.ubc.ca (P. Reyad).

https://doi.org/10.1016/j.aap.2019.05.029
Received 16 February 2019; Received in revised form 12 April 2019; Accepted 29 May 2019
Available online 06 June 2019

The original models are conflict-based SPFs for signalized intersections. These SPFs relate rear-end conflicts occurring in each signal cycle to dynamic variables such as traffic volume, maximum queue length, shock wave characteristics, and platoon ratio. The models were developed based on actual traffic data extracted from video scenes recorded at six signalized intersections in Canada. The Time-to-Collision (TTC) (Hayward, 1972) was used as a traffic conflict indicator. The regression results showed that the models have good fit with all explanatory variables being statistically significant (Essa and Sayed, 2018a).

In this study, the transferability analysis included evaluating the performance of the real-time safety models, presented in (Essa and Sayed, 2018a), at two new jurisdictions. Several conventional measures of transferability and goodness-of-fit were estimated. Moreover, the SPFs were locally calibrated at the new jurisdictions and their transferability was re-evaluated after the calibration process. The overall goal was to test the validity of using those SPFs for real-time safety evaluation at signalized intersections.

2. Related work

2.1. Safety models for signalized intersections

Safety models, also usually known as safety performance functions (SPFs), are regression models that correlate quantitatively the expected number of collisions with traffic exposure and geometric characteristics of road facilities. SPFs of signalized intersections have been widely developed, investigated and calibrated in the literature. The Highway Safety Manual (HSM) (AASHTO, 2010) provides various SPFs that estimate the average crash frequency for signalized intersections on different road classes including rural two-lane roads, rural multi-lane roads, urban and suburban arterials. Several studies developed and calibrated collision-based SPFs for signalized intersections to suit local conditions of specific jurisdictions (Poch and Mannering, 1996; Miaou and Lord, 2003; Lyon et al., 2005; Wang et al., 2006; Wong et al., 2007; Wang and Abdel-Aty, 2008; Guo et al., 2010; Persaud et al., 2012; Lee et al., 2017). The traffic exposure measure used in most of these studies was an aggregation of the traffic volume (e.g. AADT) and the predicted number of collisions was usually aggregated to several years. To overcome some of the limitations associated with the use of collision data in safety analysis, other studies developed SPFs for signalized intersections on the basis of field-observed traffic conflicts (Sayed and Zein, 1999; El-Basyouny and Sayed, 2013; Zhang et al., 2014; Sacchi and Sayed, 2016a, 2016b). In these studies, the exposure measure is usually represented by the average hourly traffic volume, while traffic conflicts are usually aggregated to hours (i.e. number of conflicts/hour). However, due to traffic data aggregation and the lack of including dynamic traffic variables, neither the collision-based SPFs nor the conflict-based SPFs are feasible for real-time safety evaluation.

To enable real-time safety evaluation, various real-time safety models were introduced in the literature. However, most of previous research has focused on real-time crash risk analysis for freeways (Lee et al., 2003; Pande and Abdel-Aty, 2006; Hossain and Muromachi, 2012; Ahmed and Abdel-Aty, 2013; Xu et al., 2013; Shi and Abdel-Aty, 2015; Wu et al., 2017b; among others). A few studies have considered the real-time safety analysis for signalized intersections and urban arterials (e.g., Theofilatos, 2017; Theofilatos et al., 2017; Yuan and Abdel-Aty, 2018; Yuan et al., 2018). Most of these studies investigated the relationship between the potential crash risk and real-time traffic and weather characteristics at signalized intersections in a time period shorter than one hour, generally 5–15 min. Essa and Sayed (2018a, Essa and Sayed, (2018a, 2018b) used a time period shorter than 5 min when developing conflict-based SPFs for signalized intersections. Specifically, the time period was considered to be the signal cycle length (roughly ranging from 1 to 2 min). The developed SPFs relate the number of rear-end conflicts to various real-time traffic characteristics such as the traffic volume, the shock wave area, and the platoon ratio (Essa and Sayed, 2018a, 2018b).

2.2. Transferability of SPFs

Many previous studies have examined transferring and calibrating collision-based SPFs from one jurisdiction to another. Several approaches were proposed in the literature to calibrate the transferred safety models locally at the destination jurisdiction. For example, the HSM (AASHTO, 2010) presents a calibration procedure to adjust the predictive SPFs which was developed with data from one jurisdiction for application in another jurisdiction. The procedure aims to account for differences between jurisdictions in factors such as climate, driver populations, etc. In this procedure, the baseline SPFs should be first modified by collision modification factors (CMFs) to account for differences in features from the baseline conditions, such as the lane width for two-lane roads or the existence of left-turn lane at signalized intersections. Afterwards, a calibration factor (C) should be applied to adjust the number of the predicted collisions at the new jurisdiction. As shown in Eq. (1), the calibration factor (C) is the ratio of the total observed crash frequencies for a selected set of sites at the new jurisdiction to the total predicted crash frequencies for the same sites, during the same time period (AASHTO, 2010).

$$C = \frac{\sum Observed\ Crashes}{\sum Predicted\ Crashes} \quad (1)$$

The HSM calibration procedure has been applied in many previous studies in different jurisdictions for different types of road facilities. Table 1 provides a sample of these studies with their description.

Although it was applied widely in the literature, the HSM's calibration procedure was criticized by some researchers for several reasons. First, the procedure does not provide a method for testing the model transferability. Moreover, there is no evidence to show that the calibration procedure accounts for the safety differences between various regions. Thus, the procedure may lead to inaccurate estimations and predictions when applied to some jurisdictions, especially outside the United States, due to the large variation in the general level of crash frequencies and the risk factors that vary between jurisdictions. Lastly, the HSM's calibration procedure is an aggregate method that does not correct for the errors in the predicted crashes of individual locations (Sawalha and Sayed, 2006a; Persaud et al., 2002; Chen et al., 2012; Cunto et al., 2014; Farid et al., 2018).

To overcome the limitations of the HSM's procedure, several approaches have been proposed in previous research for calibrating the transferred SPFs locally at the new jurisdiction. This includes the intercept and over-dispersion parameter calibration (Sawalha and Sayed, 2006a), the Bayesian Modelling Averaging (Chen et al., 2012), the calibration function for the Negative Binomial distribution of collisions (Srinivasan et al., 2016), the Modified Empirical Bayes (Farid et al., 2016), the informative priors (Farid et al., 2017), and the local regression (Farid et al., 2018), among others.

To assess the goodness-of-fit of the transferred models, various statistical measures have been applied in the literature. This includes cumulative residual (CURE) plots (Persaud et al., 2002; Chen et al., 2012; Sacchi et al., 2012; Cunto et al., 2014); the transfer index (Hadayeghi et al., 2006; Farid et al., 2016, 2018); the Pearson chi-squared and Z-score (Sawalha and Sayed, 2006a; Cunto et al., 2014); the mean prediction bias, the mean absolute deviation, and the mean absolute percentage error (Chen et al., 2012; Sacchi et al., 2012; Cunto et al., 2014; Farid et al., 2016, 2018).

In this study, the transferability of the real-time SPFs developed in (Essa and Sayed, 2018a) was investigated. The calibration procedure proposed by (Sawalha and Sayed, 2006a) was applied to transfer the SPFs to new jurisdictions. The procedure comprises a local calibration at the destination jurisdiction for both the model's intercept and the over-dispersion parameter (the shape parameter of the Negative

Table 1
Sample of Previous Studies that Adopted the HSM's Calibration Procedure.

Study	Country	Road Facility	C
(Srinivasan and Carter, 2011)	USA, NC	Rural 2-Lane, Signalized Intersections 4-Leg	1.04
		Rural 4-Lane, Signalized Intersections 4-Leg	0.49
		Urban 2-Lane, Signalized Intersections 3-Leg	2.47
		Urban 2-Lane, Signalized Intersections 4-Leg	2.79
(Xie et al., 2011)	USA, OR	Rural 2-Lane Undivided, Road segments	0.74
		Rural Multi-Lane Undivided, Road segments	0.36
		Rural Multi-Lane Divided, Road segments	0.78
		Urban 2-Lane Undivided, Road segments	0.63
		Rural 4-Leg Signalized Intersections	0.15
		Urban 3-Leg Signalized Intersections	0.75
		Urban 4-Leg Signalized Intersections	1.10
(Brimley et al., 2012)	USA, UT	Rural 2-way 2-Lane, Road segments	1.16
(Young et al., 2012)	Canada, SK	Urban 3-Leg Unsignalized Intersections	1.47
		Urban 4-Leg Unsignalized Intersections	1.63
		Urban 3&4-Leg Signalized Intersections	2.25
(Mehta and Lou, 2013)	USA, AL	Rural 2-way 2-Lane, Road segments	1.392
		Rural 4-Lane Divided, Road segments	1.103
(Sun et al., 2014)	USA, MO	Rural Multi-Lane Divided, Road segments	0.98
		Urban 2-Lane Undivided, Road segments	0.84
		Urban 4-Lane Divided, Road segments	0.98
		Urban 5-Lane Undivided, Road segments	0.73
		Urban 3-Leg Signalized Intersections	3.03
		Urban 4-Leg Signalized Intersections	4.91
(Cafiso et al., 2012) & (D'agostino, 2014)	Italy	Rural Multi-Lane Divided, Road segments	1.26
(Cunto et al., 2014)	Brazil	Urban Signalized Intersections	0.98
		Urban Unsignalized Intersections	2.15

Binomial model). To test the model transferability, the transfer index (Koppelman and Wilmot, 1982) was applied. Furthermore, several goodness-of-fit measures were used to assess the model fit at the new jurisdictions. This includes: 1) the Pearson's product moment correlation coefficient; 2) the mean prediction bias; 3) the mean absolute deviation; 4) the mean absolute percentage error; 5) the Pearson chi-squared (Pearson, 1900); and 6) the Z-score (Vogt and Bared, 1998).

3. Data preparation

Three datasets were prepared and used to investigate the transferability of the real-time conflict-based SPFs from their base jurisdiction to two destination jurisdictions. The datasets consist of hundreds of traffic signal cycles. At each signal cycle, the space-time diagram was plotted using real vehicle trajectories and actual signal timings; then different traffic parameters were extracted. The extracted traffic parameters include: the traffic volume, the maximum queue length, the shock wave area and speed, the platoon ratio, and the number of rear-end conflicts. Fig. 1 shows an example of the space-time diagram of one signal cycle and illustrates the extracted traffic parameters.

3.1. Base jurisdiction dataset

The dataset presented in (Essa and Sayed, 2018a) was utilized as the base jurisdiction for the transferability analysis. The data was obtained from traffic videos recorded at six signalized intersections located in the City of Edmonton and the City of Surrey in Canada. High-resolution video cameras (29.97 frames per second) were installed at each intersection to capture traffic videos. At each intersection, the video camera was fixed on an existing post located either downstream the stop line or upstream the functional area of the traffic signal. The camera scenes were generally focused on the intersection approaches where most of rear-end conflicts occur. The distance along the intersection approach covered by the video camera ranges from 110 to 130 m. Table 2 (Essa and Sayed, 2018a) provides details on the selected intersections including: the intersected roads, the date and time of data collection, the selected approaches, the number of lanes per approach, and the signal timing.

The video data was analyzed in (Essa and Sayed, 2018a) to track vehicles and extract their trajectories. Detailed trajectories of more than 2500 vehicles were extracted. The procedure starts with identifying actual traffic signal timing and cycles for each intersection by detecting the changes in the signal colors from video scenes using a MATLAB code. At each video frame, the code identifies the traffic signal indicator (e.g. green, red, or yellow) by detecting the RGB (red-green-blue) values of the signal head. Afterwards, vehicle trajectories in through lanes were obtained using another MATLAB code. The code detects the RGB values at each frame for a number of points (e.g. 50 or 100 points) located along the centerline of the studied lane. Next, a linear transformation was conducted to convert vehicle trajectories from the 3D coordinate system of the video image into the 2D coordinate system of the orthographic image (Google Satellite image) (Ismail et al., 2013). Using the converted vehicle trajectories and the signal timing, the space-time diagram for each cycle was plotted. More details on the video analysis procedure can be found in (Essa and Sayed, 2018a). From the space-time diagram, various traffic parameters and the number of rear-end conflicts at each cycle were estimated. Table 3 (Essa and Sayed, 2018a) provides a summary of statistics of the base jurisdiction dataset used in the transferability analysis.

3.2. Destination jurisdiction datasets

Two different datasets, from two corridors of signalized intersections in California and Atlanta in USA, were used as destination jurisdictions for the transferability analysis. For each corridor, detailed traffic data was obtained from the NGSIM vehicle trajectories and supporting data provided online by the United States Department of Transportation (US DOT, 2018). The first corridor is Lankershim Boulevard, an arterial in Los Angeles, California, USA. Vehicle trajectories for three main intersections along this corridor were analyzed. The second corridor is Peachtree Street, an arterial in Atlanta, Georgia, USA. Vehicle trajectories for four main intersections along this corridor were analyzed. Fig. 2 shows the location and the selected intersections of both corridors. Details on the selected intersections along each corridor are provided in Table 4. This includes: the intersected roads, the date and time of data collection, the selected approaches, the number of

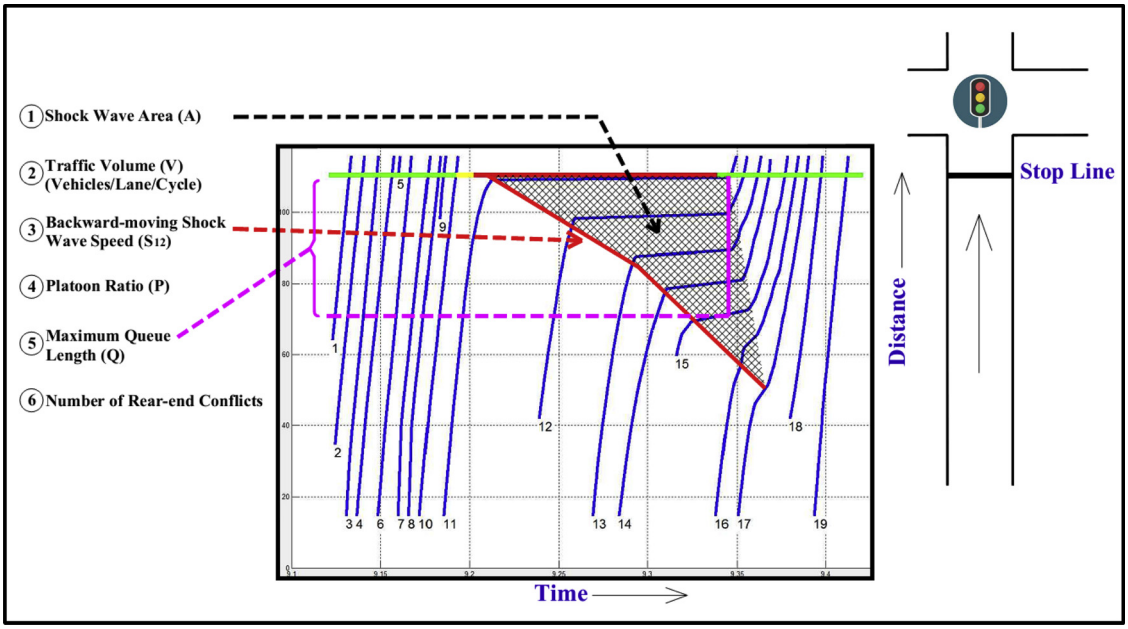

Fig. 1. *: Space-time Diagram with Traffic Characteristics Selected for the SPFs.
*Edited from the original figure provided by (Essa and Sayed, 2018b).

lanes per approach, and the signal timing.

The NGSIM data was originally collected by researchers for the NGSIM program through a network of synchronized digital video cameras. NGVIDEO, a customized software application developed for the NGSIM program, transcribed the vehicle trajectory data from the video (US DOT, 2018). For the analysis of this paper, the trajectory data for each of the selected corridors was downloaded from (US DOT, 2018) as a spreadsheet. The spreadsheet includes vehicles' identification number, position, length, occupied lane number, speed, direction, and acceleration at each 0.1 s for 30-minutes period. A MATLAB code was developed to filter the NGSIM data for each intersection approach and divide it into cycles. For each cycle, the code plots the space-time diagram to determine different traffic characteristics and the number of rear-end conflicts. Detailed trajectories of more than 2100 vehicles were extracted and analyzed. Table 5 provides a summary of statistics of the first and the second destination jurisdiction datasets.

4. SPFs at the signal cycle level

4.1. Explanatory variables

The explanatory variables of the developed SPFs represent dynamic traffic characteristics that can affect the occurrence of traffic conflicts at the signal cycle level. The traffic variables described in the following paragraphs were determined for each signal cycle. It is noteworthy to mention that only through-lanes were considered in the analysis. Exclusive left-turn and right-turn lanes were excluded. Also, all of these traffic characteristics were measured only for cycles that are under-saturated. Over-saturated cycles, where a vehicle can stay in the same approach for more than one cycle, were not included in this study. Future research is recommended to consider over-saturated flow when evaluating safety at the cycle level.

The first two explanatory variables of the developed SPFs are the exposure measure represented by the traffic volume (**V**) per cycle per lane and the maximum queue length (**Q**) at each cycle. The third explanatory variable is the platoon ratio (**P**). The platoon ratio is defined in the Highway Capacity Manual (AASHTO, 2000) as the proportion of all vehicles arriving during green multiplied by the ratio of the signal cycle length to the effective green time of the subject movement. The platoon ratio and the arrival type were shown in previous studies to have a significant effect on the frequency of rear-end conflicts at signalized intersections (Essa and Sayed, 2015a, 2015b, 2016). For each cycle, the platoon ratio was measured assuming that the effective green time is the green time plus half of the yellow time.

The last two explanatory variables represent two shock wave characteristics: the shock wave area (**A**) and the backward-moving shock wave speed ($\mathbf{S_{12}}$) (as shown in Fig. 1**)**. These shock wave characteristics were chosen based on their significant effect on the frequency of rear-end conflicts at signalized intersections (Essa and Sayed, 2018a). The relationship between shock waves and road safety has also been proven in previous studies (Chatterjee and Davis, 2016; Zheng et al., 2010; Machiani and Abbas, 2016).

4.2. Model response

The model response in the developed SPFs is the number of traffic conflicts per cycle. Only rear-end conflicts at the intersection approaches were considered. Time-to-Collision (TTC) was used as a traffic conflict indicator. TTC is generally recognized as the most frequently used indicator to identify rear-end conflicts. The TTC is defined as "*the time required for two vehicles to collide if they continue at their present speeds and on the same path*" (Hayward, 1972). For each constitutive vehicle trajectories moving in the same lane, the TTC can be continuously estimated over time using the following equation.

$$TTC_t = \frac{X_{L,t} - X_{F,t} - D_L}{V_{F,t} - V_{L,t}}\ ;\ \forall\ (V_{F,t} - V_{L,t}) > 0 \quad (2)$$

Where:

t: Time interval
L: Leading vehicle
F: Following Vehicle
X: Vehicle position
V: Vehicle speed
D: Vehicle length

Using the minimum TTC of each conflict, the number of rear-end conflicts was determined for each signal cycle. Selecting a specific TTC threshold to determine the number of rear-end conflicts was an issue. In the literature, there is a lack of agreement on what is the critical TTC threshold value that can be used to discriminate between conflict and non-conflict events. Hirst and Graham (Hirst and Graham, 1997)

Table 2
* Description of the Study Locations (Base Jurisdiction Dataset, Canada).

Site #	City (Province)	Intersected roads	Video-data was recorded in	Selected approaches	Number of Lanes per approach	Traffic signal timing (s)
1	Edmonton (AB)	Stony Plain Rd & 170 St	May 27th, 2015 (2:00 – 3:00 pm) & June 2nd, 2015 (2:00 – 3:00 pm)	170 St (Northbound)	1 (Left), 4 (Through), 1 (Right)	Red: 51, Yellow: 4, Green: 65
2	Edmonton (AB)	Gateway Blvd & 34 Ave	May 26th, 2015 (3:00 – 4:00 pm)	Gateway Blvd (Northbound)	1 (Left), 4 (Through), 1 (Right)	Red: 53 to 73, Yellow: 4, Green: 43 to 53
3	Surrey (BC)	72 Ave & 128 St	March 28th, 2012 (10:00 – 11:00 am) & March 29th, 2012 (2:00 – 3:00 pm)	72 Ave (Eastbound & Westbound)	1 (Left), 1 (Through), 1 (Through + Right)	Red: 31 to 57, Yellow: 4, Green: 29 to 64
4	Surrey (BC)	72 Ave & 132 St	April 3rd, 2012 (9:00 – 10:00 am)	72 Ave (Westbound)	1 (Left), 1 (Through), 1 (Through + Right)	Red: 17 to 49, Yellow: 4, Green: 37 to 69
5	Surrey (BC)	64 Ave & King George Blvd	June 10th, 2015 (1:00 – 2:00 pm) & June 11th, 2015 (1:00 – 2:00 pm)	King George Blvd (Southbound)	1 (Left), 2 (Through), 1 (Right)	Red: 43 to 76, Yellow: 4, Green: 34 to 66
6	Surrey (BC)	Fraser Highway & 168 A St	June 10th, 2015 (9:00 – 10:00 am) & June 11th, 2015 (9:00 – 10:00 am)	Fraser Highway (Southbound)	1 (Left), 1 (Through), 1 (Through + Right), 1 (Bike lane)	Red: 27 to 60, Yellow: 4, Green: 50 to 81

* Edited from the original table provided by (Essa and Sayed, 2018a).

Table 3
Summary of Base Jurisdiction Dataset Statistics (Canada) (Essa and Sayed, 2018a).

Variable	Description	Unit	Mean	SD	Min	Max
V	Traffic Volume per lane per cycle	–	11.58	3.56	2	22
A	Shock wave area	km. seconds	1.05	0.96	0	3.93
Q	Maximum queue length	meter	40.42	24.54	0	97.46
S12	Backward-moving shock wave speed	meter/second	−2.07	2.65	−27.2	0
P	Platoon ratio	–	1.26	0.40	0	2.27
TTC1.5	Number of rear-end conflicts (TTC ≤ 1.5 sec)	–	1.88	1.88	0	7

reported that a TTC of 4 s could be used to distinguish between dangerous and non-dangerous situations. Hogema and Janssen (1996) mentioned that the critical TTC threshold, in a driving simulator experiment, is 3.5 and 2.6 s for non-supported and supported drivers, respectively (Hogema and Janssen, 1996; Minderhoud and Bovy, 2001). The TTC threshold of 1.50 s is commonly used by researchers to define rear-end conflicts (van der Horst and Hogema, 1993). In this paper, the critical TTC threshold of 1.50 s was applied. However, using more than one TTC threshold is recommended as a future research to provide SPFs that can address different conflict-severity levels.

4.3. Model development

The SPFs were developed using the generalized linear models (GLM) approach. The GLM approach was widely applied in literature for the development of collision and conflict prediction models (e.g., Sawalha and Sayed, 2001; El-Basyouny and Sayed, 2013; Persaud et al., 2010). Previous studies showed that the number of potential traffic conflicts related to the number of vehicles arriving within a small time-interval at a road site occurs by a Poisson process (Elvik et al., 2103). Assuming that traffic conflicts are non-negative, discrete, and rare events compared to the circulating traffic volume, mixed-Poisson distribution family might be used in this regard as with crash data (Sacchi and Sayed, 2016b). The GLM approach used to model traffic conflict occurrence assumes an error structure that follows Poisson or Negative Binomial (Poisson-Gamma) distribution. Generally, the model must yield logical results. That is, it must predict zero values of conflict frequency for zero values of exposure variable (i.e. traffic volume), as well as it must not lead to a negative number of conflicts. A commonly used model form consists of an exposure measure(s) raised to some power and multiplied by an exponential function incorporating the remaining explanatory variables. Such a model form can be linearized by the logarithm link function (Sawalha and Sayed, 2006b; Essa and Sayed, 2018a). The real-time SPFs in this research can be expressed mathematically as follows (Essa and Sayed, 2018a):

$$E(Y) = V^{a_1} \exp\left[a_0 + \sum_j a_j x_j\right] \quad (3)$$

Where:

$E(Y)$: The predicted number of rear-end conflicts per cycle;

V: The traffic volume per lane per cycle (exposure);

x_j: Any other explanatory variables (such as A, Q, S12, or P);

a_0, a_1, a_j: The model parameters.

In order to decide whether the error structure follows Poisson or Negative Binomial distribution, the methodology introduced by (Sawalha and Sayed, 2006b) was applied. Poisson distribution is first assumed and the model parameters are estimated. Then the dispersion parameter (σ_d) is calculated using the following equation:

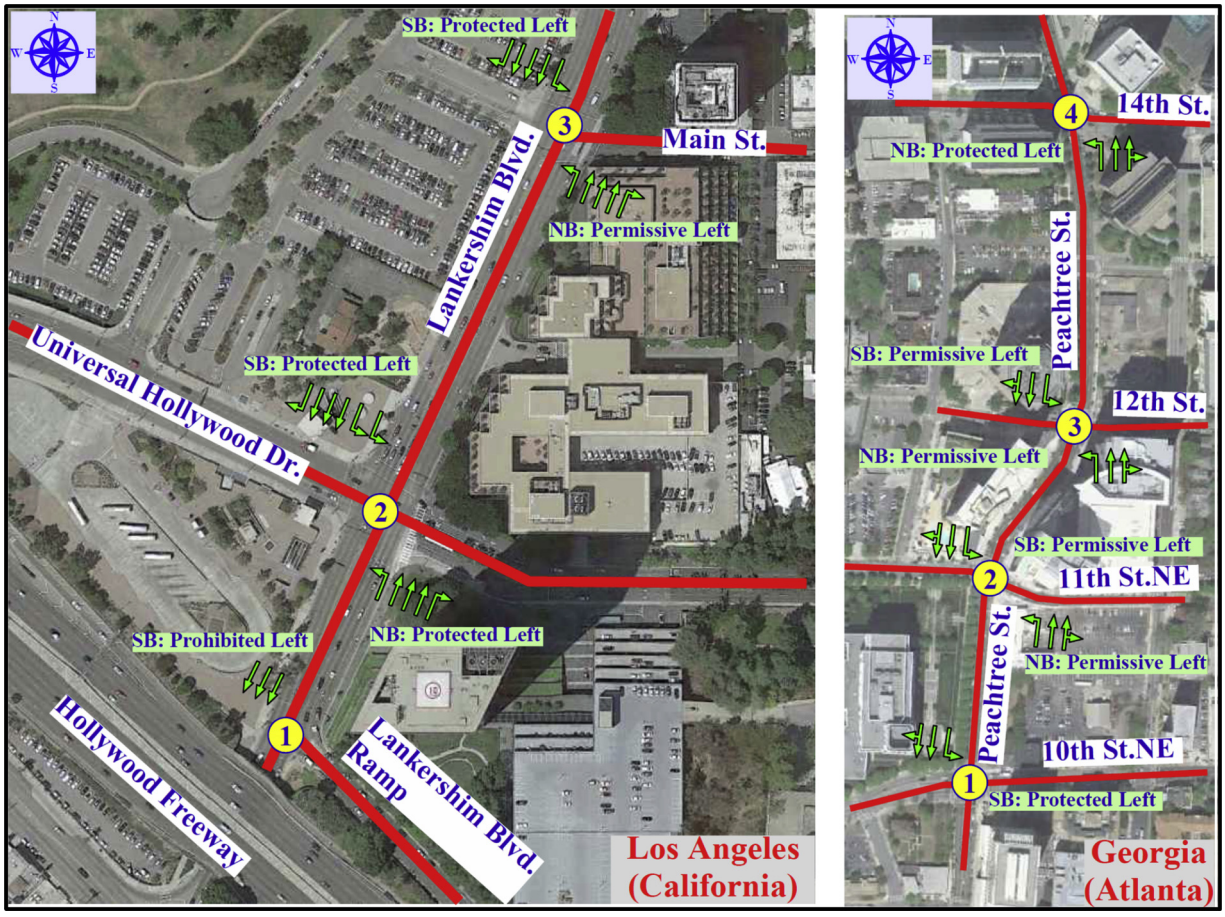

Fig. 2. Destination Jurisdictions.

$$\sigma_d = \frac{Pearson\,\chi^2}{n - p} \tag{4}$$

Where:

n: The number of observations;

p: The number of model parameters.

$Pearson\,\chi^2$ is defined as follows:

$$Pearson\,\chi^2 = \sum_{i=1}^{n} \frac{[y_i - E(Y_i)]^2}{Var(Y_i)} \tag{5}$$

Where:

y_i: The observed number of rear-end conflicts at cycle (i);

$E(Y_i)$: The predicted frequency of rear-end conflicts at cycle (i) as obtained from the conflict prediction model;

$Var(Y_i)$: The variance of conflict frequency for the cycle (i).

The dispersion parameter (σ_d) is a useful measure for assessing the amount of variation in the observed data. If the estimated value of (σ_d) is significantly greater than 1.0, this means that the data have a greater dispersion than what can be explained by the Poisson distribution, and then the Negative Binomial distribution provides a better fit to the data (Sawalha and Sayed, 2006b).

The scaled deviance (SD) and the Pearson chi-squared (χ^2) were used as statistical measures to assess the goodness of fit of the developed GLM models. Generally, for a well-fitted model with a relatively large number of observations, the expected values of (χ^2) and SD are approximately equal to the number of degrees of freedom (df) (Sawalha and Sayed, 2001). In addition, different developed models were compared using Akiake's Information Criterion (AIC) (Akaike, 1974) which can be estimated as per Eq. (**6**).

$$AIC = 2p - 2(LogLik_{full}) \tag{6}$$

Where:

p: The number of model parameters;

$LogLik_{full}$: Log-likelihood for the full model.

5. Base models (Canada)

The SPFs developed in (Essa and Sayed, 2018a) were used as the base models whose transferability needs to be investigated. These SPFs are six different models developed from the base jurisdiction dataset (Canada) using different combinations of the explanatory variables (**V**, **A**, **Q**, $\mathbf{S_{12}}$, and **P**). The reason behind developing various models was to investigate the impact of adding different explanatory variables, and to make the proposed approach applicable in different situations where the availability of measuring or estimating some explanatory variables is limited (Essa and Sayed, 2018a). Table 6 provides a summary of the base SPFs developed in (Essa and Sayed, 2018a) at the base jurisdiction (Canada).

As per Table 6, the base models show good fit with all the explanatory variables are statistically significant. Based on the estimated value of the dispersion parameter (σ_d), the error structure was assumed to follow Negative Binomial distribution for four models, and Poisson distribution for two models. The shock wave area, the maximum queue length, the shock wave speed, and the platoon ratio were shown to be important characteristics that affect the number of rear-end conflicts at the signal cycle. Incorporating one of these characteristics or a combination of them, along with the traffic volume, in the conflict-based SPFs improves the model fit and provides a better prediction of the conflict occurrence beyond what can be expected from the traffic volume only.

Table 4
Location of the Two Destination Jurisdictions.

First Destination Jurisdiction Dataset (California, USA)						
Site #	City(State)	Intersected roads	Video-data was recorded in	Selected approaches	Number of Lanes per approach	Traffic signal timing (s)
1	Los Angeles (California)	Lankershim Blvd & Lankershim Blvd Ramp	June 16th, 2005 (8:28 – 9:00 am)	Lankershim Blvd. (Southbound)	3 (Through)	Red: 15 to 30, Yellow: 3, Green: 65 to 85
2	Los Angeles (California)	Lankershim Blvd & Universal Hollywood Dr	June 16th, 2005 (8:28 – 9:00 am)	Lankershim Blvd. (Northbound & Southbound)	1 NB or 2 SB (Left), 3 (Through), 1 (Right)	Red: 32 to 77, Yellow: 3, Green: 30 to 70
3	Los Angeles (California)	Lankershim Blvd & Main St	June 16th, 2005 (8:28 – 9:00 am)	Lankershim Blvd. (Northbound & Southbound)	1 (Left), 3 (Through), 1 (Right)	Red: 17 to 33, Yellow: 3, Green: 59 to 120
Second Destination Jurisdiction Dataset (Atlanta, USA)						
Site #	City (State)	Intersected roads	Video-data was recorded in	Selected approaches	Number of Lanes per approach	Traffic signal timing (s)
1	Atlanta (Georgia)	Peachtree St & 10th St NE	November 8th, 2006 (12:45 – 1:00 pm) & (4:15 – 4:30 pm)	Peachtree St. (Southbound)	1 (Left), 1 (Through), 1 (Through + Right)	Red: 45 to 63, Yellow: 4, Green: 30 to 44
2	Atlanta (Georgia)	Peachtree St & 11th St NE	November 8th, 2006 (12:45 – 1:00 pm) & (4:15 – 4:30 pm)	Peachtree St. (Northbound & Southbound)	1 (Left), 1 (Through), 1 (Through + Right)	Red: 15 to 52, Yellow: 4, Green: 40 to 88
3	Atlanta (Georgia)	Peachtree St & 12th St NE	November 8th, 2006 (12:45 – 1:00 pm) & (4:15 – 4:30 pm)	Peachtree St. (Northbound & Southbound)	1 (Left), 1 (Through), 1 (Through + Right)	Red: 16 to 33, Yellow: 4, Green: 60 to 89
4	Atlanta (Georgia)	Peachtree St & 14th St NE	November 8th, 2006 (12:45 – 1:00 pm) & (4:15 – 4:30 pm)	Peachtree St. (Northbound)	1 (Left), 1 (Through), 1 (Through + Right)	Red: 14 to 59, Yellow: 4, Green: 31 to 84

Table 5
Summary of Statistics - Destination Jurisdiction Datasets.

First Destination Jurisdiction Dataset (California, USA)						
Variable	Description	Unit	Mean	SD	Min	Max
V	Traffic Volume per lane per cycle	–	12.70	4.04	3	26
A	Shock wave area	km. seconds	1.45	1.16	0	4.41
Q	Maximum queue length	meter	44.26	26.75	0	113.63
S12	Backward-moving shock wave speed	meter/second	−1.54	1.22	−7.60	0
P	Platoon ratio	–	1.11	0.38	0.31	2.83
TTC1.5	Number of rear-end conflicts (TTC ≤ 1.5 sec)	–	2.95	2.51	0	12
Second Destination Jurisdiction Dataset (Atlanta, USA)						
Variable	Description	Unit	Mean	SD	Min	Max
V	Traffic Volume per lane per cycle	–	8.55	3.33	1	19
A	Shock wave area	km. seconds	1.02	0.89	0	3.79
Q	Maximum queue length	meter	33.34	21.48	0	88.61
S12	Backward-moving shock wave speed	meter/second	−1.89	1.59	−6.61	0
P	Platoon ratio	–	1.37	0.60	0.20	3.68
TTC1.5	Number of rear-end conflicts (TTC ≤ 1.5 sec)	–	2.39	1.89	0	8

Table 6
Conflict-based SPFs at the Cycle Level Developed in (Essa and Sayed, 2018a).

Base models developed from the base jurisdiction dataset (Canada)							
Model# $^{*}E(Y)$=	Variables	Error Structure	K	SD	df	χ^2	AIC
One Variable (Exposure only): **Model 1:** $V^{1.563}exp(-3.231)$	*V*	NB	3.05	249	220	356	775
(Exposure + One Variable): **Model 2:** $V^{0.706}exp(-1.797 + 0.501A)$	*V, A*	NB	14.9	244	219	241	702
Model 3: $V^{0.65}exp(-2.046 + 0.0122Q)$	*V, Q*	NB	8.73	243	219	253	716
Model 4: $V^{1.637}exp(-3.316 + 0.05S_{12})$	*V,* S_{12} **	NB	3.10	248	219	347	775
Model 5: $V^{1.571}exp(-1.768 - 1.266P)$	*V, P*	Poisson	–	276	219	281	706
Combined Model: **Model 6:** $V^{1.239}exp(-1.624 + 0.294A - 0.828P + 0.119S_{12})$	*V, A, P,* S_{12}	Poisson	–	240	217	215	674

K: Shape parameter for Negative Binomial family.
All variables are significantly different from zero at 95% confidence level.
* Y: Number of rear-end conflicts per cycle with TTC equal or less than 1.50 s.
** Significantly different from zero at 90% confidence level.

6. Transferability analysis

6.1. Statistical measures to test transferability

The transferability of the base models was investigated using the data obtained from the destination jurisdictions. To assess the transferability of each model, the transfer index (TI) measure (Koppelman and Wilmot, 1982) was estimated. The Transfer Index (TI) is a relative measure that indicates how well a transferred model performs in predicting the application dataset relative to a model locally-estimated at the application context (Koppelman and Wilmot, 1982). The index has been applied in several studies to perform transferability analysis (Hadayeghi et al., 2006; Sikder et al., 2014; Farid et al., 2016, 2018). The upper bound of TI is 1, which means the transferred model performs on the new jurisdiction dataset (the application dataset) as good as the locally-estimated model. Negative values of TI indicate that the transferred model is worse than the local constant model. The TI can be expressed as follows (Koppelman and Wilmot, 1982; Hadayeghi et al., 2006):

$$TI = \frac{L_j(\hat{\theta}_i) - L_j(\hat{c})}{L_j(\hat{\theta}_j) - L_j(\hat{c})} \tag{7}$$

Where:

TI: *Transfer Index*

$L_j(\hat{\theta}_i)$: Log-likelihood in application context *j* using model from context *i*

$L_j(\hat{\theta}_j)$: Log-likelihood given by application context model *j*

$L_j(\hat{c})$: Log-likelihood given by constant model estimated in application context *j*

In addition to TI, several goodness-of-fit (GOF) measures were calculated to assess the ability of the transferred models to predict traffic conflicts at the new jurisdictions (the application jurisdictions). This includes: 1) Akiake's Information Criterion (AIC) (Akaike, 1974); 2) Pearson's product moment correlation coefficient (r); 3) Mean prediction bias (MPB); 4) Mean absolute deviation (MAD); 5) Mean absolute percentage error (MAPD); 6) Pearson chi-squared (χ^2) (Pearson, 1900); and 7) Z-score (Vogt and Bared, 1998). All of these measures compare the predicted conflicts obtained from the model with the observed ones at the new jurisdictions. The AIC of the transferred model can be estimated using Eq. 6 by getting the log-likelihood in the application context (the new jurisdiction dataset) using the model from the base context. The AIC measure is used to compare models that have the same dependent variable (the same response). For a certain dataset, the model that has the lowest AIC value is the best (Akaike, 1974). The Pearson's product moment correlation coefficient (r) between the observed and the predicted conflicts provides an indication on how well the model predicts the observed conflicts. The r values can range from -1 to +1. The ideal model gives r value of 1 which indicates a perfect fit.

The mean prediction bias (MPB) describes the magnitude and direction of the average bias in the subject model. The closer to zero the value of the MPB is, the better the model predicts the observed data. Positive values of MPB indicate that the model under-predicts the observed conflicts, and vice versa. The MPB can be expressed mathematically as follows:

$$MPB = \sum_{i=1}^{n} \frac{y_i - E(Y_i)}{n} \tag{8}$$

Where:

y_i: The observed number of rear-end conflicts at cycle (i) in the new jurisdiction dataset;

$E(Y_i)$: The predicted frequency of rear-end conflicts at cycle (i) in the new jurisdiction dataset as obtained from the conflict prediction model;

n: The sample size of the new jurisdiction dataset.

The mean absolute deviation (MAD) describes the average prediction error of the model. MAD values close to zero indicate that the model on average predicts the observed data well. The MAD can be defined as follows:

$$MAD = \sum_{i=1}^{n} \frac{|y_i - E(Y_i)|}{n} \tag{9}$$

The mean absolute percentage error (MAPD) describes the absolute prediction error of the model as a percentage of the total number of the observed conflict. The MAPD value close to zero indicates a good prediction of the subject model. The MAPD can be defined as follows:

$$MAPD = \frac{\sum_{i=1}^{n} |y_i - E(Y_i)|}{\sum_{i=1}^{n} y_i} \tag{10}$$

The Pearson chi-squared statistic (χ^2), given in Eq. 5, is a measure of the goodness of fit of a model to any dataset. Therefore, it can be used to test whether a certain model, developed at the base jurisdiction, can provide reliable predictions at a new jurisdiction (Sawalha and Sayed, 2006a; Vogt and Bared, 1998). The Z-score measures how far the calculated χ^2 statistic is from its expected value. Z-score values close to zero indicate that the transferred model predicts the new observed data well. The Z-score can be defined as follows (Sawalha and Sayed, 2006a; Vogt and Bared, 1998):

$$Z\_Score = \frac{\chi^2 - E(\chi^2)}{\sigma(\chi^2)} \tag{11}$$

Where:

$E(\chi^2)$: The expected value of χ^2 (the number of observations in the new dataset (n));

$\sigma(\chi^2)$: The standard deviation of χ^2.

In addition to the previous GOF measures, the HSM calibration factor (C), which is defined in Eq. 1, was estimated for each model to compare the total number of the predicted conflicts with the total number of the observed conflicts. C values higher than 1 indicate that the model generally underestimate the number of conflicts, and vice versa. However, this factor was used in this study as a GOF measure not as a calibration factor to calibrate the SPFs.

6.2. Transferability analysis approaches

Generally, there are two approaches for analyzing the transferability of a specific model: 1) the application-based approach, and 2) the estimation-based approach. In the application-based approach, the base model developed from the base jurisdiction is applied with no change (without calibration) to the destination jurisdiction (the application context) to assess how well the model predicts at the new region. In the estimation-based approach, the base model parameters estimated from the base jurisdiction data are recalibrated using the destination jurisdiction data to test whether each parameter in the model is transferable (Sawalha and Sayed, 2006a; Sikder et al., 2014). In this paper, both approaches were applied to investigate the transferability of the base SPFs.

6.2.1. Application-based approach

In this approach, the six base SPFs, developed at the base jurisdiction (Canada), were transferred as they are with no change to the new jurisdictions (California and Atlanta). The transfer index and the GOF measures were estimated for each model. Table 7 provides the results obtained from the transferred models at each destination jurisdiction.

The results in Table 7 show that the transferred models have high values of TI that range from 0.73 to 0.987. This reveals that the base SPFs developed at the cycle level are fairly transferable to other jurisdictions. The MPB and C results indicate that all models generally underestimate the observed conflicts. One exception of that is model 6, which slightly overestimates the number of conflicts at the first destination jurisdiction. The results also show medium to high correlation (r) between predicted and observed conflicts. In addition, Pearson chi-squared and Z-score values support the transferred models, except for models 5 and 6 at the second destination jurisdiction. In fact, it is very difficult to determine the best model of the six base SPFs when all the GOF measures provided in Table 7 are considered. However, it can be noticed that models 2, 3, and 6 have the best performance at the first destination jurisdiction. At the second destination jurisdiction, models 2 and 3 provide the best data fitting.

6.2.2. Estimation-based approach

In this approach, the base model parameters estimated from the base jurisdiction data are recalibrated using the destination jurisdiction data. Two methods of calibration were considered herein. The first method comprises the calibration of the model intercept and the shape parameter only, while the second method considers the calibration of all the model parameters.

6.2.2.1. Intercept and shape parameter calibration. In this section, the base SPFs, developed at the base jurisdiction (Canada), were transferred to the new jurisdictions (California and Atlanta) after calibrating both the model intercept and the shape parameter, following the calibration procedure proposed in (Sawalha and Sayed, 2006a). For each model, a new intercept and shape parameter for each model were determined using the method of maximum likelihood. The statistical analysis software "R" was used to perform the GLM regression and the maximum likelihood calculations. The coefficients of all the explanatory variables were forced to their original values obtained from the base jurisdiction. The "offset" command within the GLM regression functions in "R" was applied to perform this process. Afterwards, the transfer index and the GOF measures were estimated for each model. Table 8 provides the results obtained from the transferred models at each destination jurisdiction after the calibration process.

The results in Table 8 show that there is a notable improvement in the GOF measures for all models in general after calibrating the intercept and the shape parameter. Specifically, the measures TI, AIC, χ^2 and Z-Score were significantly improved. This is expected as the local calibration of the intercept and the shape parameter allows the transferred models to better suit local conditions at the destination jurisdictions. The intercept usually accounts for most factors outside the explanatory variables. On the other hand, for negative binomial models, the shape parameter (k) of the model determines the variability of the data around the model regression hyper-surface. This variability for the new jurisdiction dataset might be different than that for the original dataset. Furthermore, χ^2 and Z-Score values are dependent upon the shape parameter. Therefore, the shape parameter calibration is necessary and expected to improve the fit of the transferred models (Sawalha and Sayed, 2006a).

Table 7
Transferring the Base SPFs to the Destination Jurisdictions without Calibration.

Base Models (Canada's Models) Transferred without Calibration to the First Destination Jurisdiction (California – USA)

Model #	TI	AIC	r	MPB	MAD	MAPD	χ^2	Z Score	C
Model 1	0.984	517	0.34	0.75	1.91	0.65	175	2.72	1.344
Model 2	0.986	503	0.48	0.34	1.71	0.58	215	5.48	1.130
Model 3	0.909	490	0.77	0.65	1.36	0.46	133	0.97	1.284
Model 4	0.987	516	0.36	0.70	1.88	0.64	165	2.26	1.310
Model 5	0.956	523	0.47	0.26	1.77	0.60	305	10.7	1.097
Model 6	0.980	509	0.50	−0.01	1.79	0.61	235	6.98	0.997

Base Models (Canada's Models) Transferred without Calibration to the Second Destination Jurisdiction (Atlanta – USA)

Model #	TI	AIC	r	MPB	MAD	MAPD	χ^2	Z Score	C
Model 1	0.916	328	0.44	1.19	1.53	0.64	189	5.8	1.982
Model 2	0.953	312	0.52	0.95	1.31	0.55	158	5.32	1.654
Model 3	0.920	310	0.74	1.10	1.31	0.55	138	3.8	1.858
Model 4	0.892	336	0.37	1.20	1.57	0.66	214	7.07	2.011
Model 5	0.733	378	0.54	1.12	1.38	0.58	1379	57.59	1.877
Model 6	0.857	352	0.47	1.16	1.49	0.62	577	28.29	1.944

Table 8
Transferring the Base SPFs to the Destination Jurisdictions with Calibration of the Model Intercept and the Shape Parameter.

Base Models (Canada's Models) Transferred with Calibrated Intercept and Shape Parameter to the First Destination Jurisdiction (California – USA)

Model #	a_0^{c} *	K ^{c} **	TI	AIC	r	MPB	MAD	MAPD	χ^2	Z Score	C
Model 1	−2.899	3.13	0.998	486	0.34	−0.11	1.95	0.66	97	−0.79	0.964
Model 2	−1.58	3.98	0.996	471	0.48	−0.29	1.86	0.63	112	−0.08	0.910
Model 3	−1.796	Poisson	0.968	417	0.77	0.00	1.30	0.44	110	−0.22	1.000
Model 4	−3.013	3.27	0.997	486	0.36	−0.10	1.92	0.65	98	−0.75	0.968
Model 5	−1.599	2.96	0.967	501	0.47	−0.29	1.91	0.65	156	1.85	0.910
Model 6	−1.522	3.74	0.983	482	0.50	−0.33	1.90	0.64	125	0.53	0.900

Base Models (Canada's Models) Transferred with Calibrated Intercept and Shape Parameter to the Second Destination Jurisdiction (Atlanta – USA)

Model #	a_0^{c} *	K ^{c} **	TI	AIC	r	MPB	MAD	MAPD	χ^2	Z Score	C
Model 1	−2.525	10.59	0.998	271	0.44	−0.05	1.26	0.53	69	−0.33	0.979
Model 2	−1.273	16.92	0.999	261	0.52	−0.05	1.25	0.52	65	−0.62	0.979
Model 3	−1.427	Poisson	0.999	236	0.74	0.00	0.95	0.40	48	−1.84	1.000
Model 4	−2.576	6.80	0.982	280	0.37	−0.10	1.36	0.57	69	−0.3	0.960
Model 5	−1.008	3.85	0.874	324	0.54	−0.38	1.50	0.63	557	23.67	0.863
Model 6	−0.894	7.16	0.948	294	0.47	−0.16	1.28	0.54	213	8.27	0.937

* $\mathbf{a_0^c}$: Model intercept calibrated at the new jurisdiction.
** **K ^{c}**: Model shape parameter calibrated at the new jurisdiction.

As shown in Table 8, the TI values of the transferred models are much closer to 1. The TI values range from 0.874 to 0.999. This confirms that the base SPFs are considerably transferable to other jurisdictions if the intercept and the shape parameter are locally-calibrated. The MPB and C values became much closer to zero and one, respectively. The correlation (r) values are the same as Table 7. This is because the coefficients of all the explanatory variables were forced to their original values during the calibration process. Pearson chi-squared and Z-score values support the transferred models, except for models 5 and 6 at the second destination jurisdiction. It is still difficult to determine the best model of the six base SPFs when all the GOF measures provided in Table 8 are considered. However, it can be noticed again that models 2, 3, and 6 have the best performance at the first destination jurisdiction. At the second destination jurisdiction, models 2 and 3 provide the best data fitting.

6.2.2.2. Full model calibration. In this section, the six SPFs (shown in Table 6) were redeveloped at the two new jurisdictions: California and Atlanta, using the same procedure described earlier. The main goal is to confirm that the selected explanatory variables (**V, A, Q, P, S_{12}**) are important characteristics that affect the number of rear-end conflicts at the signal cycle and can provide a better prediction of the conflict occurrence beyond what can be expected from the traffic volume only. In addition, developing these models using different datasets can help in recommending the best one of them to be used for real-time safety evaluation. Table 9 (**a**,**b**) provides a summary of the SPFs redeveloped using the two destination jurisdiction datasets.

Overall, the redeveloped models at the two new jurisdictions, shown in Table 9, show good fit with almost all the explanatory variables are statistically significant. Based on the estimated value of the dispersion parameter (σ_d), the error structure was assumed to follow Negative Binomial distribution for all models except two models whose error structure follows Poisson distribution. The redeveloped models emphasize that the shock wave area, the maximum queue length, the shock wave speed, and the platoon ratio are important covariates that affect the number of rear-end conflicts. Incorporating one of these covariates or a combination of them, along with the traffic volume, in the SPFs improves the model fit and provides a better conflict prediction. This can be noticed from the improvement in the AIC value when adding one of these covariates to the traffic volume in the developed SPFs. Moreover, all the covariate coefficients have logical signs that conform to those of the base models provided in Table 6. In other words, the number of conflicts is expected to increase during signal cycles that have higher volumes, longer queues, and bigger shock waves. On the other side, it is intuitive that more vehicle-arrivals on green time lead to higher platoon ratios and less conflict probability.

It should be noted that some models were excluded from Table 9, such as models **3a**, and **4b-6b**. Basically, a model is excluded either because the model does not show an AIC value better than that obtained from another model with a smaller number of covariates, or because some covariates in the model are not statistically significant at 95% confidence level. This insignificance is usually due to the correlation between the model covariates (the multicollinearity effect). One factor that may contribute to the multicollinearity effect in the excluded models is the existing signal coordination along the selected corridors (Lankershim Boulevard and Peachtree Street). Future research is recommended to incorporate the effect of the signal coordination into real-time SPFs.

After redeveloping the SPFs at the new jurisdictions, the GOF measures were estimated for each model. Table 10 provides the GOF results for each model at each destination jurisdiction.

The results in Table 10 indicate that the GOF measures, especially AIC, r, and Z-Score, were improved after redeveloping the SPFs. Since the new models are locally developed by maximizing the likelihood function at the new jurisdictions, they are expected to provide a better fit to the new data. However, comparing to Table 8, the improvement in the GOF measures in Table 10 is slight. This means that the prediction performance of the models in Table 8 at the new jurisdictions is still good. Therefore, calibrating only the intercept and the shape parameter seems sufficient to transfer the base SPFs to new jurisdictions.

With regard to the models shown in Tables 9 and 10, it can be noticed that models 2 and 6 have the best performance at the first destination jurisdiction; while models 2 and 3 provide the best data fitting at the second destination jurisdiction.

7. Recommended real-time safety evaluation model

Although all the developed SPFs show a good fit with statistically significant explanatory variables and high transfer indices, it is useful to recommend a specific model for real-time safety evaluation. Based on the transferability analysis results and considering the base jurisdiction as well as the two destination jurisdictions, **model 2** is the most recommended model. **Model 2** includes two explanatory variables to predict rear-end conflicts: the traffic volume (**V**), and the shock wave area (**A**). The model is recommended due to several reasons. First, the inclusion of the shock wave area as an explanatory variable in the SPF is

Table 9
SPFs at the Cycle Level Developed at the Destination Jurisdictions.

a.Models redeveloped at the first destination jurisdiction (California - USA)

Model# $^{*}E(Y)$=	Variables	Error Structure	K	SD	df	χ^2	AIC
One Variable (Exposure only): **Model 1a:** $V^{1.067}exp(-1.633)$	*V*	NB	3.46	129	112	99	482
(Exposure + One Variable): **Model 2a:** $V^{0.625}exp(-1.049 + 0.316A)$	*V, A*	NB	6.21	128	111	113	459
Model 3a: This model was excluded	*V, Q*	–	–	–	–	–	–
Model 4a: $V^{1.232}exp(-1.853 + 0.13S_{12})$	*V,* S_{12}	NB	3.70	129	111	99	481
Model 5a: $V^{0.987}exp(-0.937 - 0.461P)$	*V, P*	NB	4.14	132	111	106	478
Combined Model**: **Model 6a:** $V^{0.805}exp(-1.295 + 0.32A + 0.143S_{12})$	*V, A,* S_{12}	NB	7.01	127	110	110	456

b.Models redeveloped at the second destination jurisdiction (Atlanta - USA)

Model# $^{*}E(Y)$=	Variables	Error Structure	K	SD	df	χ^2	AIC
One Variable (Exposure only): **Model 1b:** $V^{1.116}exp(-1.531)$	*V*	NB	19.8	80	72	69	268
(Exposure + One Variable): **Model 2b:** $V^{0.924}exp(-1.49 + 0.307A)$	*V, A*	Poisson	–	74	71	65	255
Model 3b: $V^{0.483}exp(-1.078 + 0.023Q)$	*V, Q*	Poisson	–	55	71	47	236
Model 4b: This model was excluded	*V,* S_{12}	–	–	–	–	–	–
Model 5b: This model was excluded	*V, P*	–	–	–	–	–	–
Combined Model: **Model 6b:** This model was excluded	*V, A, P,* S_{12}	–	–	–	–	–	–

K: Shape parameter for Negative Binomial family.
All variables are significantly different from zero at 95% confidence level.
* Y: Number of rear-end conflicts per cycle with TTC equal or less than 1.50 s.
** The platoon ratio (**P**) was removed from this model as it was not statistically significant at 95% confidence level.

logical. Considering the shock wave area enables the SPF to discriminate between different cycles even if the traffic volume is the same. Basically, at a specific traffic volume, cycles with bigger shock waves most likely are expected to cause more conflicts. In addition, the shock wave area can describe, indirectly, the maximum queue length and the vehicle arrival pattern. Most importantly, the shock wave area is affected by the signal timing. Therefore, the effects of real-time signal changes on traffic conflicts can be captured in the real-time SPF through the shock wave area.

Second, **model 2** shows a good fit at the three studied jurisdictions. The explanatory variables of the model (**V** and **A**) are statistically significant at 95% confidence level. The model has AIC value that is significantly lower than that of the exposure-only model (**model 1**). This means that the model provides a better prediction of the conflict occurrence beyond what can be expected from the traffic volume only.

Third, **model 2** shows high transfer indices, 0.986 and 0.953, at the two new jurisdictions. These indices have further improved to 0.996 and 0.999 after calibrating the intercept and the shape parameter. The high values of the TI confirm the transferability of the model among different contexts. Furthermore, the other GOF measures of **model 2** at the new jurisdictions affirm the model transferability. As shown in Tables 7–10, the model shows r values range from 0.48 to 0.59, Z scores range from -0.62 to 5.48, C values close to 1, scaled deviance and χ^2 values close to the degree of freedom, and MPB and MAD values close to zero. However, it should be noted that calibrating the intercept and the shape parameter is important to improve the model fit when

Table 10
Goodness-of-Fit Measures of SPFs Developed at the Destination Jurisdictions.

Full Model Calibration at the First Destination Jurisdiction (California – USA)

Model #	AIC	r	MPB	MAD	MAPD	χ^2	Z Score	C
Model 1a	482	0.35	−0.01	1.87	0.63	99	−0.72	0.997
Model 2a	459	0.52	−0.02	1.61	0.55	113	−0.05	0.992
Model 3a	–	–	–	–	–	–	–	–
Model 4a	481	0.38	−0.01	1.8	0.61	99	−0.72	0.997
Model 5a	478	0.45	0.00	1.78	0.60	106	−0.41	1.001
Model 6a	456	0.54	−0.02	1.58	0.54	110	−0.19	0.993

Full Model Calibration at the Second Destination Jurisdiction (Atlanta – USA)

Model #	AIC	r	MPB	MAD	MAPD	χ^2	Z Score	C
Model 1b	268	0.47	0.00	1.24	0.52	69	−0.36	0.998
Model 2b	255	0.59	0.00	1.13	0.47	65	−0.61	1.000
Model 3b	236	0.74	0.00	0.94	0.39	47	−1.92	1.000
Model 4b	–	–	–	–	–	–	–	–
Model 5b	–	–	–	–	–	–	–	–
Model 6b	–	–	–	–	–	–	–	–

transferring to new jurisdictions.

Finally, the regression results of **model 2** are consistent at the three jurisdictions (Tables 6 and 9**a, b**) in terms of the sign and the value of the model parameters. As logically-expected, the signs of the traffic volume (**V**) and the shock wave area (**A**) coefficients are positive when **model 2** is developed at any of the three jurisdictions. The coefficient of the traffic volume (a_1) is 0.706, 0.625, and 0.924 at the base jurisdiction, the first destination jurisdiction, and the second destination jurisdiction, respectively. All the (a_1) values are consentient to be less than 1, meaning that the projection of the model function in the **Y-V** plane concaves down. The coefficient of the shock wave area (a_2) has consistent positive values that range from 0.307 to 0.501.

8. Conclusion

This paper investigates the transferability of the conflict-based real-time SPFs of signalized intersections that were developed in (Essa and Sayed, 2018a). The SPFs relate various dynamic traffic parameters to the number of rear-end conflicts at the signal cycle level. The traffic parameters include: the traffic volume, the maximum queue length, the shock wave speed and area, and the platoon ratio. To investigate the models' transferability, two corridors of signalized intersections in California and Atlanta states were used in the analysis as destination jurisdictions. Detailed vehicle trajectories for these corridors were obtained from the NGSIM data. Two transferability analysis approaches were applied: 1) the application-based approach, and 2) the estimation-based approach. In the first approach, the base models were applied with no change (without calibration) to the destination jurisdictions to assess how well the models predict at the new region. In the second approach, the model parameters estimated from the base jurisdiction data were recalibrated using the destination jurisdiction data. Two methods of calibration were conducted. The first method comprises the calibration of the model intercept and the shape parameter only, while the second method considers the calibration of all the model parameters.

In both transferability approaches, the transfer index (TI) measure was estimated to test the transferability of the base SPFs. Additionally, several goodness-of-fit (GOF) measures were examined to assess and compare the prediction performances of the transferred models at the destination jurisdictions. The applied GOF measures are: 1) Akiake's Information Criterion (AIC); 2) Pearson's product moment correlation coefficient (r); 3) Mean prediction bias (MPB); 4) Mean absolute deviation (MAD); 5) Mean absolute percentage error (MAPD); 6) Pearson chi-squared (χ^2); and 7) Z-score.

Overall, the results showed that the conflict-based real-time SPFs are fairly transferable among different sites. The transfer index ranged from 0.73 to 0.987 when the base SPFs were transferred without calibration and from 0.874 to 0.999 when the intercept and the shape parameter were calibrated. Also, the transferred SPFs generally, with and without calibration, were shown to have a good fit for the destination jurisdiction datasets. The GOF results indicated medium to high correlation between the predicted conflicts and the observed ones, small Z scores, and MPB and MAD values close to zero. However, there was a notable improvement in the GOF measures for all models in general after calibrating the intercept and the shape parameter. Specifically, the measures AIC, χ^2 and Z-Score were significantly improved. This is expected as the local calibration of the intercept and the shape parameter allows the transferred models to better suit local conditions at the destination jurisdictions.

In the second calibration method, the base SPFs were redeveloped at the destination jurisdictions. All the model parameters were estimated by the GLM approach using the new jurisdictions datasets. The results showed that the redeveloped models have good fit with almost all the explanatory variables are statistically significant. The redeveloped models emphasize that the shock wave area, the maximum queue length, the shock wave speed, and the platoon ratio are important covariates that affect the number of rear-end conflicts. Incorporating one of these covariates or a combination of them, along with the traffic volume, in the SPFs improves the model fit and provides a better conflict prediction. Moreover, all the covariate coefficients had logical signs; this means the number of conflicts is expected to increase during signal cycles that have higher volumes, longer queues, bigger shock waves, and lower platoon ratios.

The GOF measures, especially AIC, r, and Z-Score, were improved after redeveloping the SPFs in the second calibration method. This is reasonable because the new models are locally developed by maximizing the likelihood function using the new data from the destination jurisdictions, which leads to a better fit. However, comparing to the first calibration method, the improvement in the GOF measures was slight. This means that calibrating only the intercept and the shape parameter seems sufficient to transfer the base SPFs to new jurisdictions.

The last contribution of this paper was to recommend one of the studied SPFs for real-time safety evaluation. Based on the transferability analysis results and considering the base jurisdiction as well as the two destination jurisdictions, the model that combined the traffic volume and the shock wave area was the most recommended model due to several reasons. First, the inclusion of the shock wave area as an explanatory variable in the SPF is logically valid. The covariate shock wave area enables the SPF to discriminate between different cycles even at the same traffic volume, and describes indirectly the maximum queue length and the vehicle arrival pattern. Most importantly, the effects of real-time signal changes on traffic conflicts can be captured in the real-time SPF through the shock wave area. Second, the recommended model showed a good fit at the three studied jurisdictions. The explanatory variables of the model are statistically significant at 95% confidence level. The model has AIC value that is significantly lower than that of the exposure-only model. Third, the recommend model shows high transfer indices, 0.986 and 0.953, at the two destination jurisdictions. These indices have further improved to 0.996 and 0.999 after calibrating the intercept and the shape parameter. Furthermore, the GOF measures at the new jurisdictions affirm the model transferability. Finally, the regression results of the recommended model are consistent at the three jurisdictions in terms of the sign and the value of each model parameter.

In conclusion, the results of this paper confirm the validity of using the conflict-based real-time SPFs developed in (Essa and Sayed, 2018a) for real-time safety evaluation of signalized intersections. This paves the way for several applications in the CVs environment, where real-time information on vehicle positions and trajectories will be available. One of these applications is the real-time safety optimization of traffic signals. In such an application, CVs data can be used to adapt signal controllers in real-time to minimize traffic conflicts and maximize safety. Future areas of research may include developing a methodology for such a safety optimization process.

Lastly, it should be noted that this study has some limitations which can be summarized as follows:

1) The sample size of the trajectory data for the base jurisdiction as well as the two destination jurisdictions was limited.
2) The SPFs in this study are applicable only to under-saturated signal cycles. Over-saturated cycles, where a vehicle can stay in the same approach for more than one cycle, were not considered in this research and should be considered in future work.
3) Only rear-end conflicts at the intersection approaches were considered. Other types of traffic conflict within the intersection area such as right-angle conflicts were not considered.
4) The critical TTC threshold was assumed to be 1.50 s. Future work may include conducting a sensitivity analysis for various TTC thresholds or using more than one TTC threshold to address different conflict-severity levels.
5) The effect of signal coordination on the results was not investigated.

6) The friction between through lanes and left/right turn lanes was not considered in the analysis. The effect of this friction becomes more apparent when left/right turn lanes are oversaturated. Considering this friction in the real-time SPFs is suggested as a future area of research.

Acknowledgement

The authors gratefully acknowledge the contributions of the University of British Columbia (UBC) and the Insurance Corporation of British Columbia (ICBC) for their financial and resource commitment to this project. The authors would also like to acknowledge Maria Albitar who helped in collecting data for this research.

References

AASHTO, 2000. Highway Capacity Manual. Transportation Research Board., Washington, D.C.
AASHTO, 2010. Highway Safety Manual. Transportation Research Board., Washington, D.C.
Ahmed, M., Abdel-Aty, M., 2013. A data fusion framework for real-time risk assessment on freeways. Transp. Res. Part C Emerg. Technol. 26, 203–213.
Akaike, H., 1974. A new look at the statistical model identification. Selected Papers of Hirotugu Akaike. Springer, New York, NY, pp. 215–222.
Brimley, B., Saito, M., Schultz, G., 2012. Calibration of Highway Safety Manual safety performance function: development of new models for rural two-lane two-way highways. Transp. Res. Rec. 2279, 82–89.
Cafiso, S., Di Silvestro, G., Di Guardo, G., 2012. Application of Highway Safety Manual to Italian divided multilane highways. Procedia-Soc.Behav. Sci. 53, 910–919.
Chatterjee, I., Davis, G., 2016. Analysis of rear-end events on congested freeways by using video-recorded shock waves. Transp. Res. Rec. 2583, 110–118.
Chen, Y., Persaud, B., Sacchi, E., 2012. Improving transferability of safety performance functions by Bayesian model averaging. Transp. Res. Rec. 2280 (1), 162–172.
Cunto, F., Sobreira, L., Ferreira, S., 2014. Assessing the transferability of the Highway Safety Manual predictive method for urban roads in Fortaleza City, Brazil. J. Transp. Eng. 141 (1), 04014072.
D'agostino, C., 2014. Investigating transferability and goodness of fit of two different approaches of segmentation and model form for estimating safety performance of Motorways. Procedia Eng. 84, 613–623.
El-Basyouny, K., Sayed, T., 2013. Safety performance functions using traffic conflicts. Saf. Sci. 51, 160–164.
Elvik, R., Erke, A., Christensen, P., 2009. Elementary units of exposure. Transp. Res. Rec. (2103), 25–31.
Essa, M., Sayed, T., 2015a. Simulated Traffic Conflicts: Do They Accurately Represent Field-Measured Conflicts? Transp. Res. Rec. 2514, 48–57.
Essa, M., Sayed, T., 2015b. Transferability of calibrated microsimulation model parameters for safety assessment using simulated conflicts. Accid. Anal. Prev. 84, 41–53.
Essa, M., Sayed, T., 2016. A comparison between PARAMICS and VISSIM in estimating automated field-measured traffic conflicts at signalized intersections. J. Adv. Transp. 50 (5), 897–917.
Essa, M., Sayed, T., 2018a. Traffic conflict models to evaluate the safety of signalized intersections at the cycle level. Transp. Res. Part C Emerg. Technol. 89, 289–302.
Essa, M., Sayed, T., 2018b. Full Bayesian conflict-based models for real time safety evaluation of signalized intersections. Accid. Anal. Prev. https://doi.org/10.1016/j.aap.2018.09.017. In Press.
Farid, A., Abdel-Aty, M., Lee, J., 2018. Transferring and calibrating safety performance functions among multiple states. Accid. Anal. Prev. 117, 276–287.
Farid, A., Abdel-Aty, M., Lee, J., Eluru, N., 2017. Application of Bayesian informative priors to enhance the transferability of safety performance functions. J. Safety Res. 62, 155–161.
Farid, A., Abdel-Aty, M., Lee, J., Eluru, N., Wang, J., 2016. Exploring the transferability of safety performance functions. Accid. Anal. Prev. 94, 143–152.
Guo, F., Wang, X., Abdel-Aty, M., 2010. Modeling signalized intersection safety with corridor-level spatial correlations. Accid. Anal. Prev. 42 (1), 84–92.
Hadayeghi, A., Shalaby, A., Persaud, B., Cheung, C., 2006. Temporal transferability and updating of zonal level accident prediction models. Accid. Anal. Prev. 38 (3), 579–589.
Hayward, J., 1972. Near-miss determination through use of a scale of danger. High. Res. Rec. 384.
Hirst, S., Graham, R., 1997. The format and presentation of collision warnings. Ergon.safe. int. driver inter. 203–219.
Hogema, J., Janssen, W., 1996. Effect of Intelligent Cruise Control on Driving Behaviour. TNO Human Factors., Soesterberg, The Netherlands.
Hossain, M., Muromachi, Y., 2012. A Bayesian network based framework for real-time crash prediction on the basic freeway segments of urban expressways. Accid. Anal. Prev. 373–381.
Ismail, K., Sayed, T., Saunier, N., 2013. A methodology for precise camera calibration for data collection applications in urban traffic scenes. Can. J. Civ. Eng. 1 (40), 57–67.
Koppelman, F., Wilmot, C., 1982. Transferability analysis of disaggregate choice models. Transp. Res. Rec. 895, 18–24.
Lee, C., Hellinga, B., Saccomanno, F., 2003. Real-time crash prediction model for application to crash prevention in freeway traffic. Transp. Res. Rec. 1840, 67–77.
Lee, J., Abdel-Aty, M., Cai, Q., 2017. Intersection crash prediction modeling with macro-level data from various geographic units. Accid. Anal. Prev. 102, 213–226.
Lyon, C., Haq, A., Persaud, B., Kodama, S., 2005. Safety performance functions for signalized intersections in large urban areas: development and application to evaluation of left-turn priority treatment. Transportation Research Record. Transp. Res. Rec. 1908, 165–171.
Machiani, S., Abbas, M., 2016. Safety surrogate histograms (SSH): a novel real-time safety assessment of dilemma zone related conflicts at signalized intersections. Accid. Anal. Prev. 361–370.
Mehta, G., Lou, Y., 2013. Calibration and development of safety performance functions for Alabama: Two-lane, two-way rural roads and four-lane divided highways. Transp. Res. Rec. 2398, 75–82.
Miaou, S., Lord, D., 2003. Modeling traffic crash-flow relationships for intersections: dispersion parameter, functional form, and Bayes versus empirical Bayes methods. Transp. Res. Rec. 1840, 31–40.
Minderhoud, M., Bovy, P., 2001. Extended time-to-collision measures for road traffic safety assessment. Accid. Anal. Prev. 1 (33), 89–97.
Pande, A., Abdel-Aty, M., 2006. Comprehensive analysis of the relationship between real-time traffic surveillance data and rear-end crashes on freeways. Transp. Res. Rec. 1953, 31–40.
Pande, A., Das, A., Abdel-Aty, M., Hassan, H., 2011. Estimation of real-time crash risk: are all freeways created equal? Transp. Res. Rec. 2237 (1), 60–66.
Pearson, K., 1900. X. On the criterion that a given system of deviations from the probable in the case of a correlated system of variables is such that it can be reasonably supposed to have arisen from random sampling. The London, Edinburgh, and Dublin Philosophical Magazine and Journal of Science 302 (50), 157–175.
Persaud, B., Lan, B., Lyon, C., Bh, R., 2010. Comparison of empirical Bayes and full Bayes approaches for before–after road safety evaluations. Accid. Anal. Prev. 42 (1), 38–43.
Persaud, B., Lord, D., Palmisano, J., 2002. Calibration and transferability of accident prediction models for urban intersections. Transp. Res. Rec. 1784, 57–64.
Persaud, B., Saleem, T., Faisal, S., Lyon, C., Chen, Y., Sabbaghi, A., 2012. Adoption of highway safety manual predictive methodologies for Canadian highways. Proceedings from the 2012 Conference of the Transportation Association of Canada.
Poch, M., Mannering, F., 1996. Negative binomial analysis of intersection-accident frequencies. J. Transp. Eng. 122 (2), 105–113.
Sacchi, E., Sayed, T., 2016a. Conflict-based safety performance functions for predicting traffic collisions by type. Transp. Res. Rec. 2583, 50–55.
Sacchi, E., Sayed, T., 2016b. Bayesian estimation of conflict-based safety performance functions. J. Transp. Saf. Secur. 8 (3), 266–279.
Sacchi, E., Persaud, B., Bassani, M., 2012. Assessing international transferability of highway safety manual crash prediction algorithm and its components. Transp. Res. Rec. 2279, 90–98.
Sawalha, Z., Sayed, T., 2001. Evaluating safety of urban arterial roadways. J. Transp. Eng. 127 (2), 151–158.
Sawalha, Z., Sayed, T., 2006a. Transferability of accident prediction models. Saf. Sci. 44 (3), 209–219.
Sawalha, Z., Sayed, T., 2006b. Traffic accident modeling: some statistical issues. Can. J. Civ. Eng. 33 (9), 1115–1124.
Sayed, T., Zein, S., 1999. Traffic conflict standards for intersections. Transp. Plan. Technol. 22, 309–323.
Shew, C., Pande, A., Nuworsoo, C., 2013. Transferability and robustness of real-time freeway crash risk assessment. J. Safety Res. 46, 83–90.
Shi, Q., Abdel-Aty, M., 2015. Big data applications in real-time traffic operation and safety monitoring and improvement on urban expressways. Transp. Res. Part C Emerg. Technol. 58, 380–394.
Sikder, S., Augustin, B., Pinjari, A.R., Eluru, N., 2014. Spatial transferability of tour-based time-of-Day choice models. Transp. Res. Rec. 1 (2429), 99–109.
Srinivasan, R., Carter, D., 2011. Development of Safety Performance Functions for North Carolina (No. FHWA/NC/2010-09). North Carolina Department of Transportation, Research and Analysis Group, Chapel Hill, NC.
Srinivasan, R., Colety, M., Bahar, G., Crowther, B., Farmen, M., 2016. Estimation of calibration functions for predicting crashes on rural two-lane roads in Arizona. Transp. Res. Rec. 2583, 17–24.
Sun, C., Brown, H., Edara, P., Claros, B., Nam, K., 2014. Calibration of the HSM's SPFs for Missouri. Publication CMR14-007. Missouri Department of Transportation, Missouri.
Theofilatos, A., 2017. Incorporating real-time traffic and weather data to explore road accident likelihood and severity in urban arterials. J. Safety Res. 61, 9–21.
Theofilatos, A., Yannis, G., Vlahogianni, E., Golias, J., 2017. Modeling the effect of traffic regimes on safety of urban arterials: the case study of Athens. J. Traffic Transp. Eng. 4 (3), 240–251.
U.S. Department of Transportation, 2015. ITS Research 2015-2019: Connected Vehicle (Connected Vehicles: Benefits, Roles, Outcomes). Retrieved May 12, 2017, from. https://www.its.dot.gov/research_areas/WhitePaper_connected_vehicle.htm.
US DOT, 2018. Next Generation Simulation (NGSIM) Vehicle Trajectories and Supporting Data. Retrieved March 2018, from. US Department of Transportation. https://data.transportation.gov/Automobiles/Next-Generation-Simulation-NGSIM-Vehicle-Trajector/8ect-6jqj.
van der Horst, R., Hogema, J., 1993. Time-to-collision and collision avoidance systems. Proceedings of the 6th ICTCT Workshop.
Vogt, A., Bared, J., 1998. Accident models for two-lane rural segments and intersections. Transp. Res. Rec. 1635, 18–29.
Wang, X., Abdel-Aty, M., 2008. Modeling left-turn crash occurrence at signalized intersections by conflicting patterns. Accid. Anal. Prev. 40 (1), 76–88.
Wang, X., Abdel-Aty, M., Brady, P., 2006. Crash estimation at signalized intersections: significant factors and temporal effect. Transp. Res. Rec. 1953, 10–20.

Wong, S.C., Sze, N.N., Li, Y.C., 2007. Contributory factors to traffic crashes at signalized intersections in Hong Kong. Accid. Anal. Prev. 39 (6), 1107–1113.
Wu, Y., Abdel-Aty, M., Lee, J., 2017b. Crash risk analysis during fog conditions using real-time traffic data. Accid. Anal. Prev.
Xie, F., Gladhill, K., Dixon, K., Monsere, C., 2011. Calibration of highway safety manual predictive models for Oregon state highways. Transp. Res. Rec. 2241, 19–28.
Xu, C., Tarko, A., Wang, W., Liu, P., 2013. Predicting crash likelihood and severity on freeways with real-time loop detector data. Accid. Anal. Prev. 57, 30–39.
Xu, C., Wang, W., Liu, P., Guo, R., Li, Z., 2014. Using the Bayesian updating approach to improve the spatial and temporal transferability of real-time crash risk prediction models. Transp. Res. Part C Emerg. Technol. 38, 167–176.
Young, J., Park, P., Eng, P., 2012. Comparing the highway safety manual's safety performance functions with jurisdiction-specific functions for intersections in Regina. Annual Conference of the Transportation Association of Canada.
Yuan, J., Abdel-Aty, M., 2018. Approach-level real-time crash risk analysis for signalized intersections. Accid. Anal. Prev. 119, 274–289.
Yuan, J., Abdel-Aty, M., Wang, L., Lee, J., Wang, X., Yu, R., 2018. Real-time crash risk analysis of Urban arterials incorporating bluetooth, weather, and adaptive Signal control data. Proceedings of the Transportation Research Board 97th Annual MeetingTransportation Research Board.
Zhang, X., Liu, P., Chen, Y., Bai, L., Wang, W., 2014. Modeling the frequency of opposing left-turn conflicts at signalized intersections using generalized linear regression models. Traffic Inj. Prev. 15 (6), 645–651.
Zheng, Z., Ahn, S., Monsere, C., 2010. Impact of traffic oscillations on freeway crash occurrences. Accid. Anal. Prev. 42 (2), 626–636.